Macromolecular Research, Vol. 22, No. 7, pp 765-772 (2014)
DOI 10.1007/s13233-014-2141-7

www.springer.com/13233
pISSN 1598-5032 eISSN 2092-7673

Effect of Carbon Nanotube Functionalization on the Structure and Properties of Poly(3-hydroxybutyrate)/MWCNTs Biocomposites

Mongyoung Huh[1], Min Hae Jung[1], Young Soo Park[1], Byung-Joo Kim[1], Min Suk Kang[2], Peter J. Holden[3], and Seok Il Yun*[,4]

[1]*Korea Institute of Carbon Convergence Technology, Jeonbuk 561-844, Korea*
[2]*School of Chemical and Biological Engineering, Seoul National University, Seoul 151-742, Korea*
[3]*Australian Nuclear Science & Technology Organisation, Locked Bag 2001, Kirrawee, N.S.W., 2232, Australia*
[4]*Department of Industrial Chemistry, Sangmyung University, Seoul 110-743, Korea*

Received January 28, 2014; Revised May 21, 2014; Accepted June 10, 2014

Abstract: Multi walled carbon nanotubes (MWCNTs) covalently functionalized with an alkyl chain exhibited a better dispersion in poly(3-hydroxybutyrate) (PHB) solutions and cast films as compared with acid-treated MWCNTs (MWCNT-COOH) due to the much improved solubility in chloroform. The alkylated MWCNTs more effectively strengthened PHB composites than non-alkylated MWCNTs due to their uniform dispersion as well as stronger interaction of alkylated MWCNTs with the PHB matrix. Both acid-treated and alkylated MWCNTs added to PHB matrix facilitated crystallization kinetics. However the crystallization kinetics were found to be slower for the alkylated MWCNTs/PHB composites than acid-treated MWCNTs composites. The results may be ascribed to the inhibitory effect on PHB crystallization caused by the steric hindrance of the long alkyl chains attached to MWCNTs.

Keywords: poly(3-hydroxybutyrate), multi walled carbon nanotubes (MWCNTs), biocomposite, covalent functionalization, alkyl chain, crystallization kinetics, storage modulus.

Introduction

The world-wide use of conventional petrochemical based plastics presents two major economic and environmental issues. Firstly global petroleum reserves are being rapidly depleted leading to increased cost which will continue to have a major impact on the global economy. Secondly petrochemical plastics are non-biodegradable and the resulting toxic wastes cause serious environmental burdens. The problems associated with conventional petrochemical plastics have brought biodegradable polymers to the forefront.[1-7] Poly(3-hydroxybutyrates) (PHBs) are thermoplastic polyesters naturally synthesized by micro-organisms as storage materials in response to unbalanced growth conditions.[5-7] PHBs have similar end-use properties to petrochemical plastics (*e.g.*, polypropylene) yet are biodegradable in most biologically active circumstances including soils, oceans, compost and sewage.[5-7] The recent demonstration of production of PHB in transgenic plants such as *Arabidopsis thaliana* at low cost makes PHB a promising alternative to petrochemical plastics.[4,6,8-10] Besides high volume commercial applications, PHBs have become one of the most interesting biomaterials in the medical and pharmaceutical industries, primarily due to their excellent biodegradability and biocompatibility.[5,11,12] Nanocomposites of biopolymers with carbon nanotubes (CNTs) offer significant potential for their increased utilization, as a result of the improvements in electric conductivity, mechanical and thermal properties.[4,13-15] However the full potential of employing CNTs as reinforcements has been severely limited because of the poor dispersion and poor interfacial bonding of CNTs to polymer matrices.[16-18] These problems largely stem from the smooth surface of CNTs, which is chemically inert and incompatible with most solvents and polymers. CNT aggregation has been found to dramatically hamper the mechanical and electrical properties of composites. The weak CNTs-polymer adhesion is also unable to provide an efficient load transfer across the CNT/matrix interface. Therefore, significant efforts have been directed towards developing methods to modify surface properties of CNTs. One of the most frequently used techniques for surface modifications of CNTs is to covalently functionalize CNT surfaces.[16-23] Chemical functionalization is based on the covalent linkage of functional entities onto carbon scaffolds of CNT surfaces. The amidation or esterification of oxidized CNT has become one of the most popular ways of producing functionalized CNTs. Chen *et al.* treated oxidized nanotubes to achieve attachment of long alkyl chains to single wall carbon nanotubes (SWNTs) *via* amide linkages.[19] Further studies showed that the presence of the long alkyl

*Corresponding Author. E-mail: yunsans@smu.ac.kr

chain made CNTs soluble in organic solvents such as chloroform, tetrahydrofuran (THF) and CS_2.[20] Sun and co-workers showed that the esterification of the carboxylic acids can also be applied to functionalize CNTs.[21-23]

Recent studies demonstrates that significant reinforcements can be accomplished for composites where the matrix polymer and the polymer grafted onto the CNTs are the same or compatible, which includes the poly(*L*-lactic acid) composites containing CNTs functionalized with an alkyl chain.[24-29] Although nanocomposites of PHB/CNTs have been studied by several groups,[30-32] investigations of utilization of covalently functionalized CNTs to obtain a better dispersion of CNTs within PHB matrix has not been reported. Most of the previous studies on PHB/CNTs nanocomposites were based on CNT modified with carboxyl functional groups. In this paper we synthesized multiwall carbon nanotubes (MWCNTs) and covalently functionalized MWCNTs with a long alkyl chain. This covalent functionalization of MWCNTs has a significant impact on the structure and physical properties of PHB nanocomposites such as the crystallization behavior and mechanical properties which are discussed in this paper.

Experimental

Materials. Poly(3-hydroxybutyrate) (a number average molecular weight, M_n=2.9×10^5) was purchased from Aldrich. All reagents were purchased from TCI, JUNSEI and Aldrich. MWCNTs were produced *via* the chemical vapor deposition method and purified according to a liquid oxidation method.[33] Nitric acid (HNO_3) is the most commonly used reagent for CNT purification for its mild oxidation ability, which can selectively remove amorphous carbon and metal catalysts. Briefly 1 g of the as-prepared MWCNT sample was refluxed under magnetic stirring in 1 L of 3 M nitric acid for 2 h (acid treatment more than 2 h caused excess damage of CNTs). The nitric acid solution of CNTs was then filtered through a polytetrafluoroethylene (PTFE) membrane. The CNT solids collected on the PTFE filter were rinsed with deionized water until the pH value of the water was ~ 7 and dried at 100 ºC in a vacuum oven for 12 h. The diameter (*D*) range of purified MWCNTs was 4~6 nm which generate a relatively high aspect ratio compared to other commercial MWCNTs (*D*=10~20) (Figure 1).

Preparation of Acid-Treated/Alkylated MWCNT. The purified MWCNTs were further chemically treated to modify surfaces of CNTs as shown in Scheme I. Briefly, 5 g of the purified MWCNTs were suspended in 500 mL of concentrated nitric acid by sonication and stirred at 120 ºC for 2 h. It was reported that refluxing CNTs in concentrated nitric acid opens the ends of the CNTs and damages the walls of the SWNTs.[33] Acid treatment also introduces carboxylic acid groups at the open ends and at defect sites of CNT walls.[33] The resulting acid-treated MWCNT (MWCNT-COOH) was thoroughly washed with deionized water until the pH value of the water was ~ 6 and dried at 80 ºC in vacuum oven for 1 day. Functionalization of acid-treated MWCNTs was carried as follows.[34] 0.6 g of the MWCNT-COOH were sonicated in NaOH aqueous solution (10 mM, 900 mL) for 5 min and converted into the sodium salt form. To this black homogeneous suspension, 1 g of tetra-*n*-octylammonium bromide (TOAB) and 15 mL of alkyl bromide, 1-bromohexadecane were added in and the mixture was heated at 80 ºC for 4 h under vigorous stirring. The suspension became clear and colourless and a black precipitate was observed. The precipitate was collected and dissolved in an excess amount of chloroform ($CHCl_3$). The resulting black solid (alkylated MWCNT) was dried in a vacuum oven at 50 ºC overnight. The two different types of carbon nanotubes namely acid-treated and alkylated MWCNTs were used to make PHB composites and their structures and properties were compared.

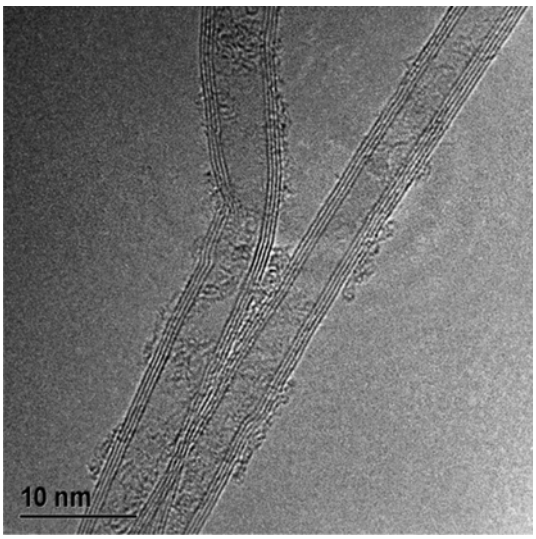

Figure 1. TEM images of the purified MWCNTs.

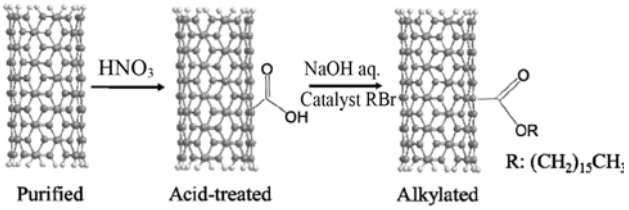

Scheme I. Functionalization of MWCNTs with an alkyl group.

Preparation of PHB/MWCNTs Nanocomposite Films. Solvent casting was used to produce neat PHB films and PHB/MWCNT composite films. Commercial PHB polymer was dissolved in chloroform (4 wt%) under stirring at 100 ºC and cooled down to the room temperature prior to casting or mixing. The MWCNTs in chloroform were sonicated for 5 min and PHB solutions were subsequently added into the MWCNT solutions. The composite solutions in chloroform were then heated to 100 ºC and cooled down to the room temperature.

The solutions were cast onto glass plates and allowed to evaporate for an hour followed by drying in vacuum oven. The glass plates were heated to 50 ºC to accelerate chloroform evaporation during the solvent casting process.

Characterization. Transmission electron microscope (TEM) micrographs of MWCNTs powder and ultrathin sections of nanocomposite films were obtained using a JEM-2200FS (JEOL KOREA LTD.) at an acceleration voltage of 200 kV. The thermal behaviors of samples were investigated using a differential scanning calorimeter (DSC, Shimadzu TA Instruments TA-60WS) and a thermogravimetric analyzer (TGA, Shimadzu TA Instruments TGA-50) under N_2 atmosphere. Dynamic mechanical analysis of nanocomposite films was performed using a TA Instrument Q800 with the tensile mode on polymeric films with a width of 3 mm and thickness in the range of 1.5 mm. A temperature scan from -20 to 130 ºC at a heating rate of 4 ºC min^{-1} was applied. A frequency of 1 Hz was used, with a static tension control of 110% and a controlled dynamic strain of 0.2%. Nitrogen was used as purge.

Results and Discussion

The TGA data was used to estimate CNT purity and the presence and concentration of organic molecules attached to CNT sidewalls. Figure 2 shows the TGA thermograms of purified and modified MWCNTs. For the purified MWCNTs, almost no noticeable weight loss was detected over the temperature range of 30~600 ºC and the residue amount at 600 ºC was estimated to be 99.5 wt%. Similarly, acid-treated MWCNTs were scarcely decomposed due to their high thermal stability with a residue of 90 wt% at 600 ºC. The TGA profile of alkylated MWCNTs demonstrates the considerable weight loss in the temperature range 200~500 ºC which corresponds to the thermal disruption of the alkyl attachments. The results indicate the high degree of MWCNT functionalization with approximately 22 wt% of alkyl chains.

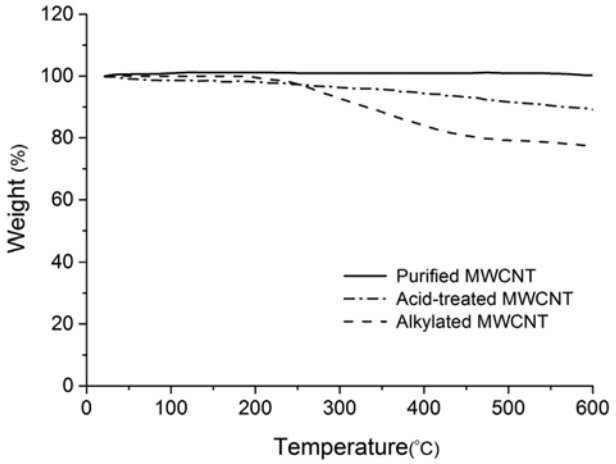

Figure 2. TGA curves of purified MWCNT, acid-treated MWCNT and alkylated MWCNT.

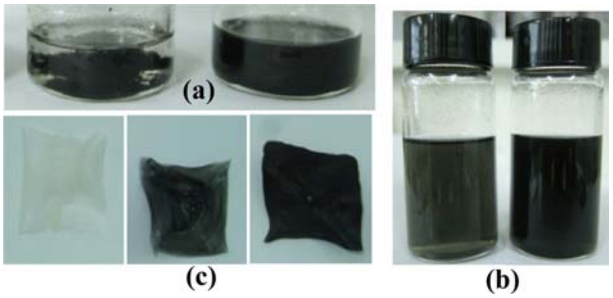

Figure 3. Comparison of CNT dispersion in (a) chloroform for acid-treated (left) and alkylated MWCNT (right) (b) polymer solutions (PHB/chloroform); acid-treated (left) and alkylated MWCNT (right) (c) cast films for neat PHB (left), acid-treated MWCNT/PHB (middle), alkylated MWCNT (right). Relative concentration of MWCNTs to PHB was 1 wt%.

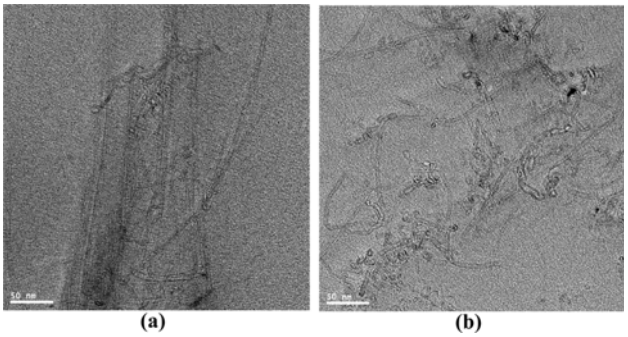

Figure 4. TEM images of PHB nanocomposite (Relative concentration of MWCNTs to PHB was 1 wt%) (a) acid-treated MWCNTs and (b) alkylated MWCNTs.

As displayed in Figure 3(a), alkylated MWCNTs exhibited better solubility in chloroform compared to acid-treated MWCNTs, which is in agreement with the previous report that alkylation of CNT surface significantly improved the solubility in chloroform.[20,34] The uniform distribution of CNTs in the solvent also resulted in better dispersion of alkylated MWCNTs in polymer solutions and cast composite films as compared to acid-treated MWCNTs (Figure 3(b), (c)). To study the homogeneity of the films, TEM was employed to investigate ultrathin sections of composite films containing surface modified MWCNTs (1 wt%). As shown in Figure 4, alkylated MWCNTs were better dispersed in PHB matrix than acid-treated MWCNTs.

The mechanical properties of the nanocomposites were analysed with dynamic mechanical analysis (DMA). The storage modulus (E') measures the energy stored during deformation and is related to the solid-like portion of polymer. The storage modulus, therefore, represents the stiffness (mechanical strength) of samples. Figure 5 compares the temperature dependence of the storage modulus (E') of neat PHB and PHB/MWCNTs. The composite films contained 1 wt% of MWCNTs. The storage modulus of all samples decreased slowly and progres-

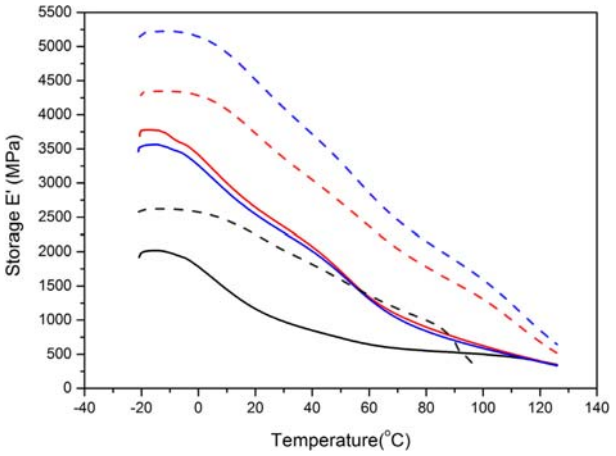

Figure 5. Storage modulus variation as a function of temperature for neat PHB and PHB/MWCNTs (relative concentration of MWCNTs to PHB was 1 wt%) composites. Black; pure PHB, Red; acid-treated MWCNTs, Blue; alkylated MWCNTs. Solid lines; before annealing (films cast and dried at 50 °C), Dotted lines; after annealing (cast films were heated at a rate of 10 °C/min up to 100 °C and maintained at 100 °C for two days).

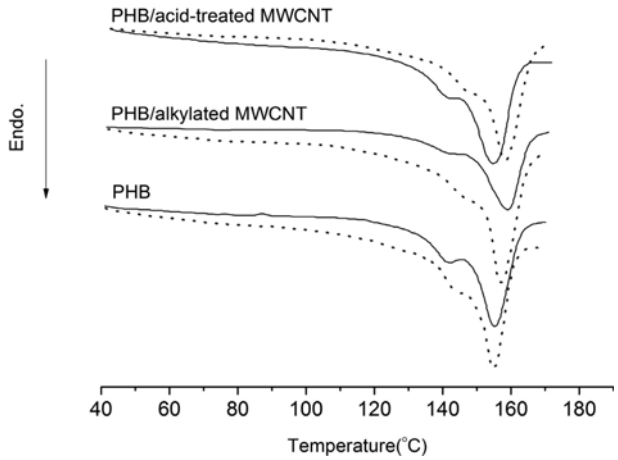

Figure 6. Thermograms of PHB/functionalized MWCNTs composites (relative concentration of MWCNTs to PHB was 1 wt%) before (solid) and after (dot) thermal annealing at 100 °C for 24 h.

Table I. Thermal Properties of Neat PHB and PHB/MWCNTs Composites before and after Thermal Annealing[a]

Samples as Cast

Type	ΔH_m (J/g)	X_c (%)	T_m (°C)
PHB	60 ± 3	40 ± 2.0	173 ± 2
PHB/Acid-treated MWCNT	64 ± 5	43 ± 3.4	171 ± 1
PHB/Alkylated MWCNT	46 ± 2	31 ± 3.4	177 ± 4

Annealed Sample

Type	ΔH_m (J/g)	X_c (%)	T_m (°C)
PHB	61 ± 4	41 ± 2.7	173 ± 1
PHB/Acid-treated MWCNT	61 ± 3	41 ± 2.0	175 ± 2
PHB/Alkylated MWCNT	66 ± 3	44 ± 1.3	175 ± 3

[a]Relative concentration of MWCNTs to PHB was 1 wt%. Uncertainty was Calculated Based on 5 Measurements for Different Sections of the Same Samples.

sively with increasing temperature, which is the typical pattern of polymers with a higher storage modulus at low temperatures (glassy state) and a lower storage modulus at high temperatures (rubbery state). In particular, the PHB nanocomposites showed higher values of E' than neat PHB over the entire temperature range showing that CNTs are effective reinforcing fillers for PHB agreeing with the previous results.[30] Unexpectedly, the higher mechanical reinforcement was not found to for alkylated MWCNTs composites which showed the better distribution of CNTs within PHB matrix. In fact, slightly smaller E' was observed for alkylated MWCNTs composites as compared with acid-treated MWCNTs composites. It has been reported that grafted CNTs inhibited polymer matrix chains from attaining a high degree of crystallinity as compared to non-grafted CNTs including pristine or acid-treated CNTs.[27,28] In general crystallization behavior of semi-crystalline polymers has a significant influence on the mechanical properties of their composites. In order to investigate the crystallinity effect on the mechanical strength for neat and PHB/MWCNTs composites, samples were heated up to 100 °C and annealed at the same temperature for sufficient time (24 h) to induce the crystallization of PHB composites. Compared to the as-cast films, the storage modulus were found to increase for annealed samples including pure PHB and the composites due to the possibly more developed crystalline phase or densification of films (Figure 6 and Table I). The storage modulus of alkylated MWCNTs composites increased more after annealing than was the case with acid-treated MWCNTs composites. To investigate the degree of crystallinity, DSC was performed on the same samples measured for DMA analysis shown in Figure 6. The degree of crystallinity, X_c (%) was determined (Table I) by measuring the enthalpy of fusion from the DSC curves shown in Figure 6 using the following equation.

$$X_c = \frac{\Delta H_m}{\Delta H^*} \times 100 \quad (1)$$

where ΔH_m is the enthalpy of fusion for the PHB samples and ΔH^* is the enthalpy of fusion for a 100% crystalline PHB which is 149.37 J/g.[35] The samples were heated from room temperature to 190 °C at a relatively higher heating rate of 40 °C/min to avoid further crystallization. Interestingly, alkylated MWCNT composites before the annealing exhibited the lowest X_c. These results show that alkyl chains grafted onto CNT surfaces disturb matrix polymers from attaining a high degree of crystallization during solvent casting process at 50 °C. Annealing did not increase the crystallinity of pure PHB and acid-treated MWCNTs composites because the solvent casting temperature (50 °C) was already high enough

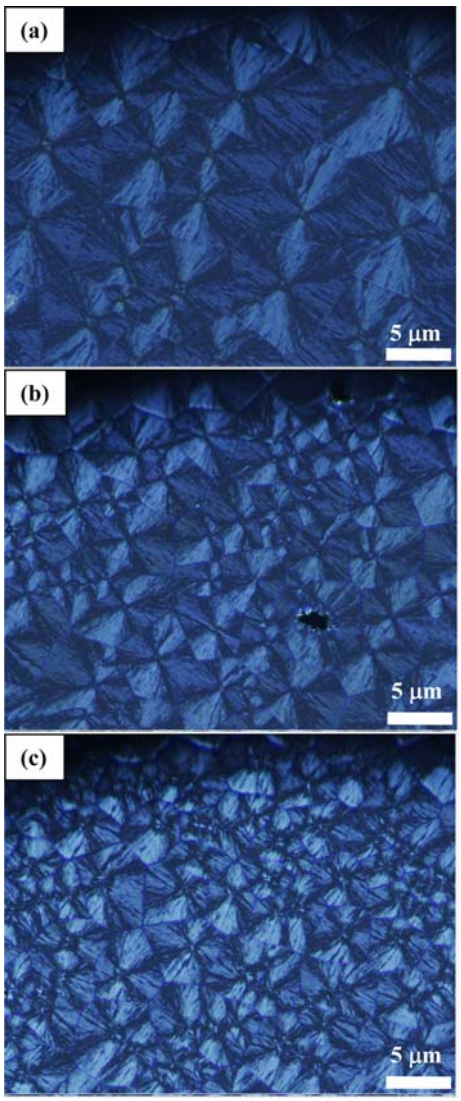

Figure 7. Polarized optical micrographs of (a) neat PHB (b) PHB/acid-treated MWCNTs (c) PHB/alkylated MWCNTs (relative concentration of MWCNTs to PHB was 0.01 wt%). The samples were spin-coated on the ITO glass with the same thickness. All the samples were annealed at 80 °C for 24 h.

to develop crystallinity. However after annealing, the crystallinity of alkylated MWCNTs composites significantly increased. All the samples exhibited a similarly high degree of crystallinity (Table I). For annealed samples, alkylated MWCNTs/PHB composites exhibited the highest value of storage modulus. The excellent mechanical strength for covalently functionalized CNT composites is attributed to homogeneous dispersion of MWCNTs in matrix as well as the strong interfacial interaction between MWCNTs and PHB matrix.

The crystalline behaviour of PHB composite films was qualitatively observed by optical microscopy measurements in cross polar mode as shown in Figure 7. The as-cast samples were annealed at 80 °C for 24 h. A large size of PHB crystalline phase with grain boundaries was observed from neat PHB (Figure 7(a)), but MWCNTs significantly reduced the PHB crystalline size (Figure 7(b), (c)) indicating that MWCNTs are excellent nucleating agents agreeing with previous results.[30] Comparing the polarized optical micrographs of PHB composites for acid-treated and alkylated MWCNTs (Figure 7(b), (c)), the alkylated composites exhibited smaller crystalline size than acid-treated MWCNTs composites. The result confirms that alkylated MWCNTs dispersed more effectively than acid-treated MWCNTs in PHB matrix resulting in more nucleating sites and smaller crystalline size as shown in Figure 7(b) and (c). To study further the effect of MWCNTs on the crystallization behavior of PHB, non-isothermal melt crystallization was investigated using DSC by heating the samples to 190 °C and annealing for 3 min to melt all the crystals previously formed, then cooling to room temperature with various cooling rates. Figure 8 shows the non-isothermal melt crystallization behaviors of neat PHB and PHB composites containing acid-treated and alkylated MWCNTs at various cooling rates. Because the samples do not have sufficient time to crystallize at a fast cooling rate, the crystallization peak temperature (T_p) shifts to the lower temperature range with increasing cooling rates for neat PHB and PHB composites. As shown in DSC thermograms (Figure 9(a)), T_p of nanocomposites shifted to a higher temperature with the incorporation of MWCNTs compared with neat PHB and T_p increased progressively with increasing MWCNTs content (Figure 9(b)). This suggests that MWCNTs are effective nucleating agents for PHB crystallization agreeing with the previous result.[30,31] From Figure 9(a), it can be also observed that PHB nanocomposites containing acid-treated MWCNTS have a bigger increase of T_p indicating better nucleating efficiency as compared to the PHB/alkylated MWCNTs nanocomposites. This unexpected findings demonstrates that the lower crystallinity found for the as-cast films of alkylated MWCNTs composites is due to the decreased nucleating efficiency during crystallization process, despite improved dispersion within the matrix, which would increase the amount of nuclei crystallizing per unit volume of the composite. The results suggest that long alkyl chains grafted onto MWCNT cause the steric hindrance to PHB crystallization resulting in the retarded nucleating efficiency and overall low crystallinity of PHB. The inhibitory effect of functionalized CNTs on the crystallization of composites has not been previously reported for PHB. However the disturbing effect for crystallization caused by grafted CNTs as compared to acid-treated (non-grafted) CNT has been reported in the literature for polyamide and poly(ether-ether-ketone) (PEEK) composites.[27,28] Generally, the inorganic fillers have two inconsistent influences on the crystallization of the semi-crystalline polymers.[36] They act as heterogeneous nucleating agents to facilitate the crystallization of polymers; on the other hand, they hinder the motion of polymer chain segments to retard the crystallization of polymers. It was concluded that the retarded crystallization is due to restricted polyamide or

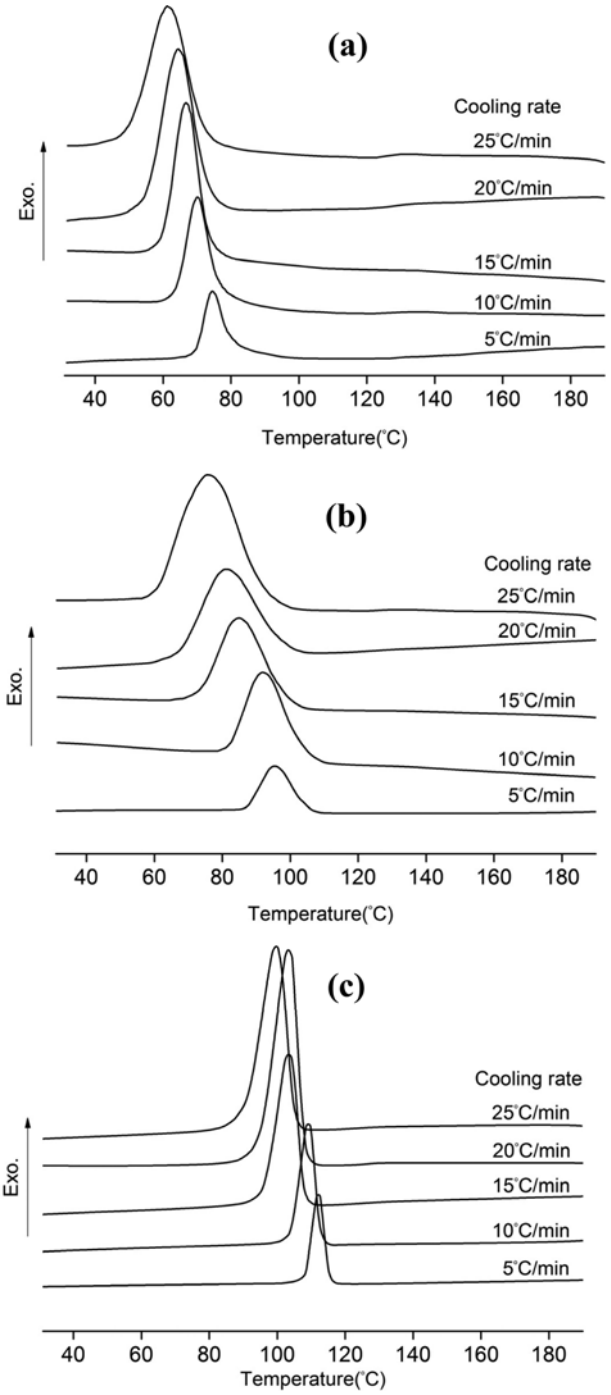

Figure 8. Non-isothermal melt crystallization behaviour of (a) neat PHB (b) PHB/acid-treated (c) PHB/alkylated MWCNTs composites at various cooling rates (composites contain 1 wt% of MWCNTs).

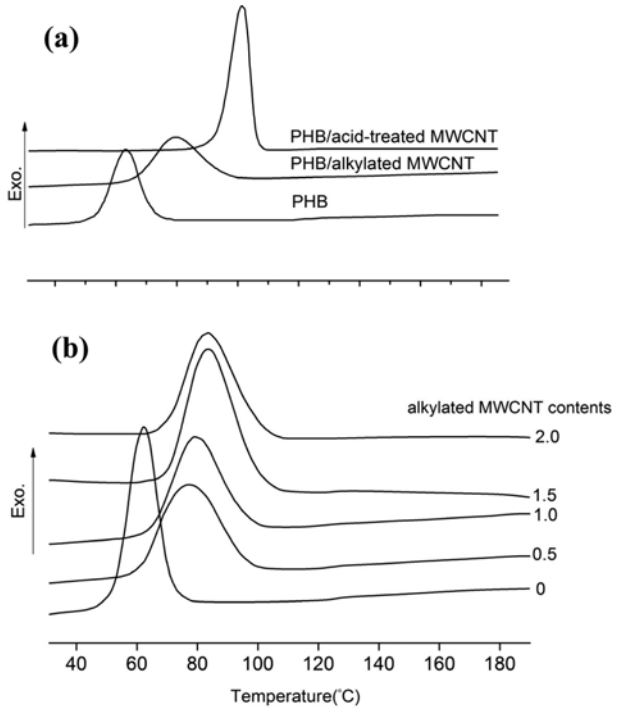

Figure 9. (a) Comparison of non-isothermal melt crystallization behavior of neat PHB and PHB composites containing 1 wt% of acid-treated and alkylated MWCNTs at a cooling rate of 20 °C/min. (b) Non-isothermal melt crystallization behaviour of PHB/alkylated MWCNTs composites containing various concentration of MWCNTs at a cooling rate of 20 °C/min.

PEEK matrix mobility caused by stronger adhesive interaction between the grafted CNT and polymers, instead of poorer nucleating efficiency found for alkylated MWCNTs in the current work. Their conclusion was based on the DSC results that grafted CNTs exhibited a bigger rise in T_p, showing more effective nucleating agents, which is opposite to the result found for the alkylated MWCNTs composites shown in Figure 8(a).

The effect of MWCNTs on the isothermal melt crystallization kinetics of PHB and composites was also characterized by DSC. The DSC measurement for melt crystallization was carried out by heating the samples to 190 °C and annealing for 3 min to melt all the crystals previously formed, then rapidly cooling to various crystallization temperatures (95~120 °C). The composite films contained 1 wt% of MWCNTs. The relative crystallinity, X_t, was determined from the area normalized to the total area. Figure 10(a) showed the typical plots of relative crystallinity as a function of crystallization time at T_c=105 °C. Crystallization time for the PHB/MWCNTs became dramatically shorter than for neat PHB. Total crystallization time of neat PHB takes almost 200 s at 105 °C, however, for PHB composites, the isothermal crystallization was much faster (7~20 s of crystallization time). The loading of MWCNTs accelerated the isothermal crystallization of PHB. The decrease of total crystallization time in the PHB composites was greater for acid-treated MWCNTs than alkylated MWCNTs, which is consistent with the inhibitory effect on the crystallization caused by long alkyl chains as discussed in the previous section. For the quantitative analysis of the isothermal crystallization kinetics, the Avrami equation was applied to the DSC data.

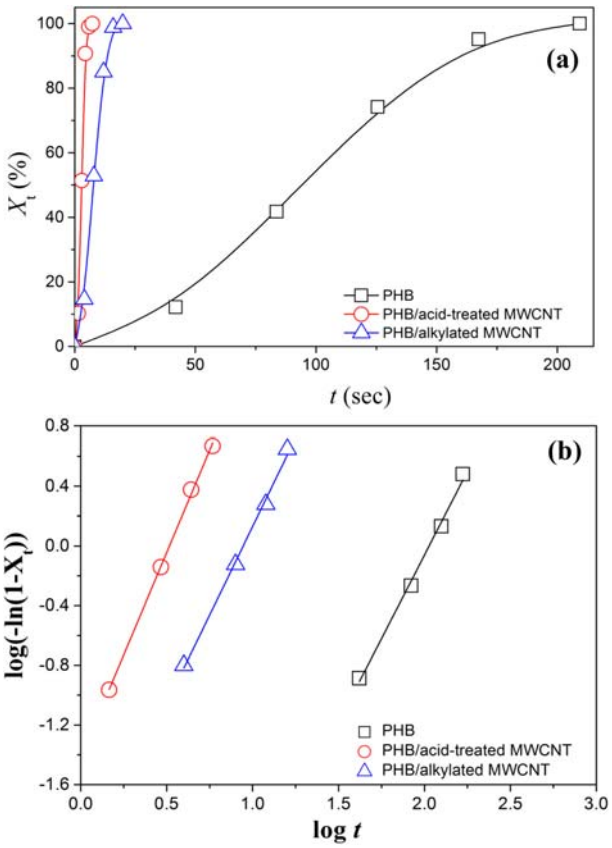

Figure 10. (a) Relative crystallinity and (b) Avrami plots as a function of crystallization time for neat PHB and PHB/MWCNTs composites containing 1 wt% of MWCNTs at T_c=105 °C.

Table II. Isothermal Melt Crystallization Kinetic Parameters for PHB and PHB/MWCNTs Composites[a]

Samples	T_c (°C)	n	k (min^{-n})
PHB	95	2.05	1.99×10^{-3}
	100	2.24	1.84×10^{-4}
	105	2.24	2.84×10^{-5}
PHB/Acid-treated MWCNT	105	2.74	3.83×10^{-2}
	110	2.68	1.30×10^{-2}
	115	2.65	9.41×10^{-4}
	120	2.54	6.13×10^{-5}
PHB/Alkylated MWCNT	105	2.37	5.72×10^{-3}
	110	2.37	7.89×10^{-4}
	115	2.31	8.71×10^{-5}
	120	2.22	1.21×10^{-5}

[a]Relative concentration of MWCNTs to PHB was 1 wt%.

The relative crystallinity X_t varies with crystallization time t as follows.[37]

$$1 - X_t = \exp(-kt^n) \quad (2)$$

where k is the crystallization rate constant and n, the Avrami exponent, is related to the nucleation mechanism and crystal growth. Figure 10(b) illustrates typical Avrami plots of PHB and PHB/MWCNTs at T_c=105 °C. The Avrami parameters, n and k were obtained from the slopes and intercepts of Avrami plots, respectively. Table II summarizes the obtained Avrami parameters at various T_c. The values of k decreased with increasing T_c because the decreased super-cooling makes more difficult for the crystallization of PHB and PHB composites. According to Table II, the k values at the same T_c (=105 °C) substantially increased in the MWCNT composites, indicating the effective nucleation for PHB melt isothermal crystallization by CNTs. The k values for the acid-treated MWCNTs composites are larger than those of alkylated MWCNTs at all T_c due to the retarded nucleation behaviour for the alkylated MWCNTs, which is consistent with the previous discussion in the current paper. The n values for neat PHB are close to 2 indicating that PHB chains tend to take the two-dimensional growth mechanism. The n values close to 2 were also reported in a previous study on pure PHB.[31] Most of the MWCNTs/PHB composites exhibited n values of 2.2~2.8 agreeing with previous results for PHB/MWCNT composites.[31] It was also found that the n values for the composites are apt to increase, approaching to 3 with increasing k values (decreasing T_c). The n value of 3 is normally attributed to thermal nucleation followed by three-dimensional crystallization growth. The transition of n values of PHB/MWCNTs nanocomposites from 2.2 to 2.8 indicates that the crystal growth process change from two-dimensional crystal growth to three-dimensional or mixed two-dimensional and three-dimensional crystal growth as isothermal T_c decreased. Figure 11 shows the variation of crystallization half-time, $t_{1/2}$ with T_c for neat PHB and MWCNTs reinforced composites. The half-time is defined as the point where the relative crystallinity, X_t reaches 50%. The half-time is usually used to describe the crystallization rate. The half-time values increase with increasing T_c due to smaller super-cooling. The MWCNTs added to the PHB effectively reduced the isothermal crystallization halftime $t_{1/2}$. The halftime values

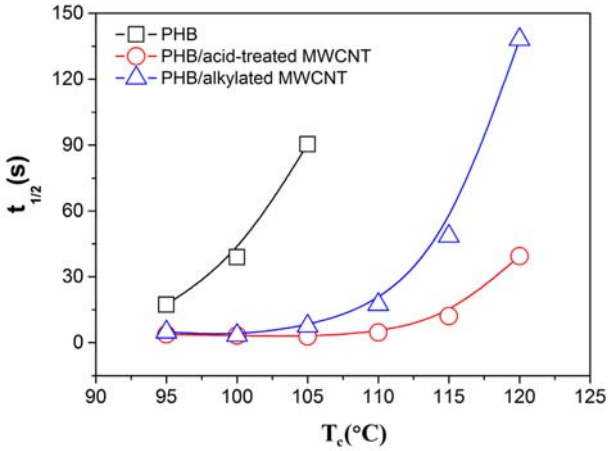

Figure 11. Temperature dependence of $t_{1/2}$ for PHB and PHB/MWCNTs composites containing 1 wt% of MWCNTs.

for alkylated MWCNTs composites were larger than acid-treated MWCNTs in the entire range of crystallization temperatures. The results clearly confirm that the steric hindrance imposed by a long alkyl chain of alkylated MWCNTs retarded the nucleation process for PHB crystallization, which resulted in the slower overall crystallization kinetics for alkylated MWCNTs composites as compared with acid-treated MWCNTs composites during the isothermal melt crystallization.

Conclusions

In this work, the effects of acid- and alkyl-modified MWCNTs on the mechanical properties and crystallization behavior of PHB were investigated. Acid treatment of MWCNTs using concentrated nitric acid as well as the further modification of acid-modified MWCNTs with alky bromide (1-bromohexandecane) was effective to graft alkyl chains to purified MWCNTs. The acid-treated MWCNTs and alkylated MWCNTs were effective reinforcements for PHB. The storage modulus was improved significantly by the incorporation of modified MWCNTs. Compared with acid-treated MWCNTs, alkylated MWCNTs had higher reinforcing efficiency for PHB, which could be attributed to the better dispersion of alkylated MWCNTs in PHB matrix. The long alkyl chains grafted onto MWCNT cause the steric hindrance to PHB crystallization resulting in the retarded nucleating efficiency and overall low crystallinity of PHB during solvent casting process. Similarly, retarded nucleation caused by a long alkyl chain of alkylated MWCNTs resulted in the slower overall crystallization kinetics for alkylated MWCNTs composites as compared with acid-treated MWCNTs composites during the isothermal melt crystallization.

References

(1) R. A. Gross and B. Kalra, *Science*, **297**, 803 (2002).
(2) A. U. B. Queiroz and F. P. Collares-Queiroz, *Polym. Rev.*, **49**, 65 (2009).
(3) G. Q. Chen and M. K. Patel, *Chem. Rev.*, **112**, 2082 (2012).
(4) M. M. Reddya, S. Vivekanandhan, M. Misra, S. K. Bhatiac, and A. K. Mohanty, *Prog. Polym. Sci.*, **38**, 1653 (2013).
(5) E. Akaraonye, T. Keshavarz, and I. Roy, *J. Chem. Technol. Biotechnol.*, **85**, 732 (2010).
(6) M. N. Somleva, O. P. Peoples, and K. D. Snell, *Plant Biotechnol. J.*, **11**, 233 (2013).
(7) C. Zhu, S. Chiu, J. P. Nakas, and C. T. Nomura, *J. Appl. Polym. Sci.*, **130**, 1 (2013).
(8) Y. Poirier, D. E. Dennis, K. Klomparens, and C. Somerville, *Science*, **256**, 520 (1992).
(9) Y. Poirier, C. Somerville, L. A. Schechtman, M. M. Satkowski, and I. Noda, *Int. J. Biol. Macromol.*, **17**, 7 (1995).
(10) Y. Poirier, *Prog. Lipid Res.*, **41**, 131 (2002).
(11) G. Q. Chen and Q. Wu, *Biomaterials*, **26**, 6565 (2005).
(12) Q. Wu, Y. Wang, and G. Q. Chen, *Artif. Cells Blood Substit. Biotechnol*, **37**, 1 (2009).
(13) P. R. Supronowicz, P. M. Ajayan, K. R. Ullmann, B. P. Arulanandam, D. W. Metzger, and R. J. Bizios, *Biomed. Mater. Res.*, **59**, 499 (2002).
(14) C. Lau, M. J. Cooney, and P. Atanassov, *Langmuir*, **24**, 7004 (2008).
(15) C. Aimé and T. Coradin, *J. Polym. Sci. Part B: Polym. Phys.*, **50**, 669 (2012).
(16) P. M. Ajayan and J. M. Tour, *Nature*, **447**, 1066 (2007).
(17) N. G. Sahoo, S. Rana, J. W. Cho, L. Li, and S. H. Chan, *Prog. Polym. Sci.*, **35**, 837 (2010).
(18) Z. Spitalsky, D. Tasis, K. Papagelis, and C. Galiotis, *Prog. Polym. Sci.*, **35**, 357 (2010).
(19) J. Chen, M. A. Hamon, H. Hu, Y. Chen, A. M. Rao, P. C. Eklund, and R. C. Haddon, *Science*, **282**, 95 (1998).
(20) M. A. Hamon, J. Chen, H. Hu, Y. S. Chen, M. E. Itkis, A. M. Rao, P. C. Eklund, and R. C. Haddon, *Adv. Mater.*, **11**, 834 (1999).
(21) J. E. Riggs, Z. Guo, D. L. Carroll, and Y. P. Sun, *J. Am. Chem. Soc.*, **122**, 587 (2000).
(22) Y. P. Sun, W. Huang, Y. Lin, K. Fu, A. Kitaygorodskiy, L. A. Riddle, Y. J. Yu, and D. L. Carroll, *Chem. Mater.*, **13**, 2864 (2001).
(23) K. Fu, W. Huang, Y. Lin, L. A. Riddle, D. L. Carroll, and Y. P. Sun, *Nano Lett.*, **1**, 439 (2001).
(24) R. Blake, J. N. Coleman, M. T. Bryne, J. E. McCarthy, T. S. Perova, W. J. Blau, A. Fonseca, J. B. Nagy, and Y. K. Gun'ko, *J. Mater. Chem.*, **16**, 4206 (2006).
(25) G. X. Chen, H. S. Kim, B. H. Park, and J. S. Yoon, *Macromol. Chem. Phys.*, **208**, 389 (2007).
(26) B. X. Yang, J.-H. Shi, K. P. Pramoda, and S. H. Goh, *Compos. Sci. Technol.*, **68**, 2490 (2008).
(27) H. Meng, G. X. Sui, P. F. Fang, and R. Yang, *Polymer*, **49**, 610 (2008).
(28) A. M. Díez-Pascual, G. Martínez, M. T. Martínez, and M. A. Gómez, *J. Mater. Chem.*, **20**, 8247 (2010).
(29) Y. S. Yun, H. I. Kwon, H. Bak, E. J. Lee, J.-S. Yoon, and H.-J. Jin, *Macromol. Res.*, **18**, 828 (2010).
(30) S. I. Yun, G. E. Gadd, B. A. Latella, V. Lo, R. A. Russell, and P. J. Holden, *Polym. Bull.*, **61**, 267 (2008).
(31) C. Xu and Z. Qiu, *Polym. Adv. Technol.*, **22**, 538 (2011).
(32) S. I. Yun, V. Lo, J. Noorman, J. Davis, R. A. Russell, P. J. Holden, and G. E. Gadd, *Polym. Bull.*, **64**, 99 (2010).
(33) P. X. Hou, C. Liu, and H. M. Cheng, *Carbon*, **46**, 2003 (2008).
(34) S. Li, Y. Qin, J. Shi, Z. X. Guo, Y. Li, and D. Zhu. *Chem. Mater.*, **17**, 130 (2005).
(35) C. Doyle, E. T. Tanner, and W. Bonfield, *Biomaterials*, **12**, 841 (1991).
(36) M. C. Kuo, J. C. Huang, and M. Chen, *Mater. Chem. Phys.*, **99**, 258 (2006).
(37) M. Avami, *J. Chem. Phys.*, **9**, 177 (1941).